

# Numerical and experimental research of the influence of hydrogen on the fracture toughness of zirconium – 2.5% niobium alloy

R. Janulionis\*, M. Daunys\*\*, G. Dundulis\*\*\*, A. Grybėnas\*\*\*\*, R. Karalevičius\*\*\*\*\*

\*Lithuanian Energy Institute, Breslaujos 3, 44403 Kaunas, Lithuania, E-mail: rjanulionis@mail.lei.lt

\*\*Kaunas University of Technology, Kęstučio 27, 44312 Kaunas, Lithuania, E-mail: mykolas.daunys@ktu.lt

\*\*\*Lithuanian Energy Institute, Breslaujos 3, 44403 Kaunas, Lithuania, E-mail: gintas@mail.lei.lt

\*\*\*\*Kaunas University of Technology, 37 Mickevieciaus str., 44244 Kaunas, Lithuania, E-mail: gintaugas.dundulis@ktu.lt

\*\*\*\*\*Lithuanian Energy Institute, Breslaujos 3, 44403 Kaunas, Lithuania, E-mail: agrybenas@mail.lei.lt

\*\*\*\*\*Lithuanian Energy Institute, Breslaujos 3, 44403 Kaunas, Lithuania, E-mail: rekara@mail.lei.lt

## 1. Introduction

Ignalina NPP unit 2 contains RBMK-1500 type reactor. Fuel channels (FC) are the major structural elements of the reactor core. The FC pressure tube Zr-2.5%Nb alloy with TMT-2 (thermomechanical treatment) is used in the NPP unit 2. The top, center and bottom segments of typical reactor fuel channels [1] are shown schematically in Fig. 1. The main component of the fuel channel is the coolant carrying tube constructed from separate end and center segments. The center segment 11 is a tube with outside diameter 88 mm (4 mm thick wall). The top 9 and bottom 15 segments are made from a stainless steel tube. The choice of zirconium alloy for the center part was made because of the relatively low thermal neutron absorption cross-section of the material and its adequate mechanical and anticorrosive properties at high temperatures (up to 350°C). The center and end pieces are joined by special intermediate coupling, made from steel-zirconium alloy.

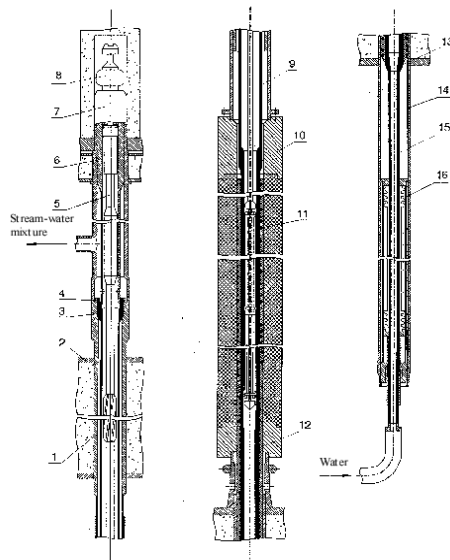


Fig. 1 Fuel channel. 1 - protective screw plug; 2 - structure "E" upper plate; 3 - FC housing in structure "E"; 4 - Leak tight weld; 5 - FA suspension unit; 6 - upper FC housing; 7 - FC cartridge; 8 - FC plug; 9 - FC upper part TK; 10 - upper steel-zirconium adapter; 11 - FC middle part; 12 - lower steel-zirconium adapter; 13 - screwed support; 14 - lower FC housing; 15 - FC lower part; 16 - compensating bellow

In case that fuel channels are the major structural elements of the reactor core the evaluation of the influence of the ageing mechanism on mechanical properties of zirconium alloys during operation of reactor is needed. The ageing mechanisms of zirconium tubes are irradiation and thermal creep causing increase of tube diameter and embrittlement of zirconium alloy under exposure of irradiation and hydrogen absorption. Hydrogen absorption by zirconium alloy during corrosion process is one of the factors determining lifetime of Zr-2.5% Nb pressure tube. When the concentration of hydrogen in material of pressure tube exceeds solubility limit [2], zirconium hydrides can be present.

The hydride is a brittle phase. The source of the embrittlement is hydride precipitates that formed as platelets. The formation of hydrides in the matrix of zirconium alloy degrades the mechanical properties of zirconium alloys: reduces ductility and resistance to brittle fracture [3-6]. Hydrides under certain conditions can cause initiation of hydride cracks (delayed hydride cracking) [7, 8]. These changes in mechanical properties need to be considered in component design-life evaluation. For this reason experimental and theoretical studies have been performed in order to understand and simulate hydride formation and its influence on zirconium alloys properties [9-13].

One of the main design and operational requirement is to preclude any unstable fracture of pressure tubes during operation. Therefore the evaluation of fracture toughness degradation due to hydrogen ingress continues to be of interest in structural integrity analysis.

The aim of this work was to study the variation of stress intensity factor of pressure tube Zr-2.5%Nb alloy with TMT-2 at different hydrogen contents. Experimentally determined mechanical properties, stress intensity factor and modeling of stress intensity factor for the nonirradiated alloy with different hydrogen concentration levels at ambient temperature were done. The computer code CASTEM 2000 was used for this analysis.

## 2. Specimens preparation and experiment

The investigation of the influence of different hydrogen concentrations on mechanical properties and fracture toughness characteristics of RBMK TMT-2 fuel channel pressure tube material has been carried out on hydrogen free specimens (it is assumed that in the initial state after production FC the content of hydrogen in the zirconium pipe comprises 0.7-3 ppm) and on the specimens

containing 45, 95 and 137 ppm hydrogen.

A ring section of Zr-2.5%Nb was cut from unirradiated RBMK TMT-2 reactor pressure tube. Sections of the pressure tube were hydrided to produce the required hydrogen concentrations using an electrolytic method and diffusion annealing treatment [14].

Hydrogen homogeneity was controlled by metallographic examination. Metallography of hydride structure sections shows a uniform hydride distribution with hydrides elongated in the longitudinal direction (Fig. 2).

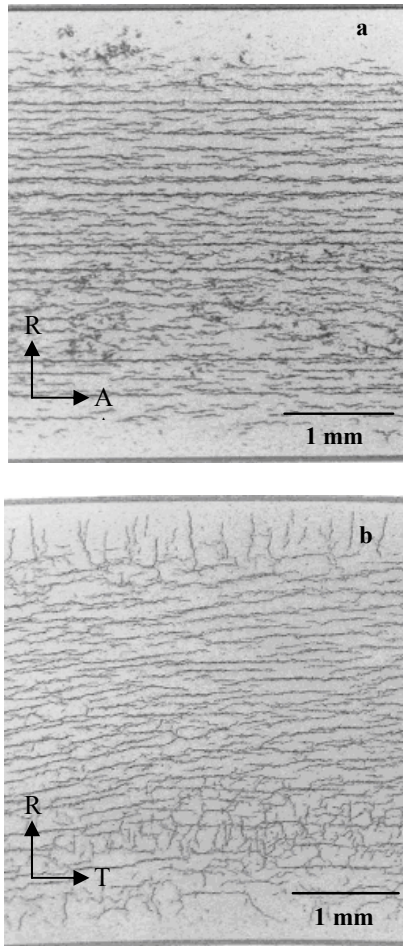


Fig. 2 Hydride microstructure of RBMK TMT-2 pressure tube material in radial – axial (a) and radial – transverse (b) sections. Hydrogen concentration of 137 ppm

Hydrogen concentrations in sections were determined using inert gas fusion method on the standard equipment LECO RH-402 using titanium with known hydrogen content as reference. Before gas analysis the section was abraded to remove the undiffused hydride layer.

Experimental results of hydrogen concentration influence on zirconium alloy mechanical characteristics and stress intensity factor, which are presented in this work, are averaged values from the set of 3-5 specimens.

Mechanical properties of RBMK pressure tube Zr-2.5%Nb alloy in TMT-2 were obtained by tension testing. As the pipe strength depends mainly on circumferential stresses, seminatural specimens in this direction from the fuel channel tube were cut off. Shape and dimensions of the specimens are shown in Fig. 3.

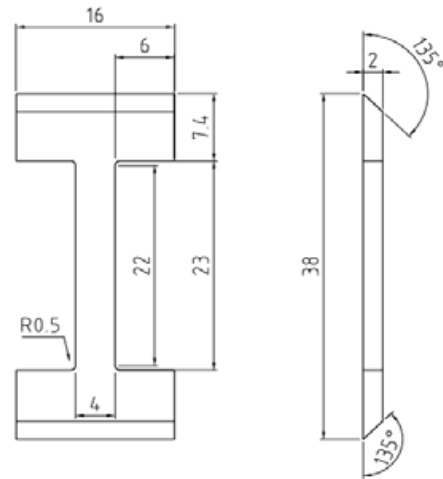


Fig. 3 Shape and dimensions of tensile specimen

The investigation was performed on the 50 kN capacity tension-compression testing machine with the stress rate  $\sigma_1 = 20$  MPa/s, which is in accordance with the requirements [3] - to keep stress loading rate in limits  $\sigma_1 = 2-20$  MPa/s. Experimental curves “force – specimen elongation” were recorded to computer via oscilloscope; load and strain values were calculated by using scales  $m_F = 10010$  N/V and  $m_e = 2.667$  mm/V.

Tensile testing and calculation technique was performed according to EN-10002-1 requirements [15].

Obtained mechanical properties for Zr-2.5%Nb alloy at ambient temperature and at different hydrogen concentration are shown in Fig. 4. The experimental data showed that increasing of hydrogen concentration causes increasing of yield stress ( $R_{p0.2}$ ), and tensile strength ( $R_m$ ), and decreasing of the relative elongation ( $A$ ). The variation of these parameters shows decrease of plasticity of this alloy.

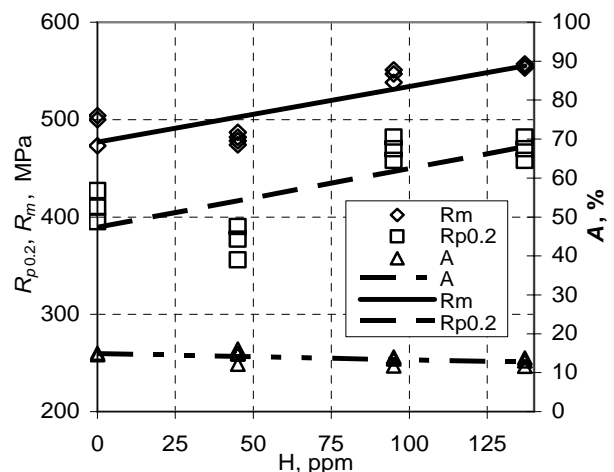


Fig. 4 Mechanical properties of Zr-2.5% Nb alloy

Fracture toughness tests have been carried out using curved compact specimens toughness. From the sections of material these specimens were machined along the axis of the pressure tube, retaining the tube curvature. Except for the thickness and the curvature of the tube, the in-plane dimensions of specimens were in proportion described for compact specimen in ASTM standard test method (E-399). Shape and dimensions of the specimen is shown in Fig. 5.

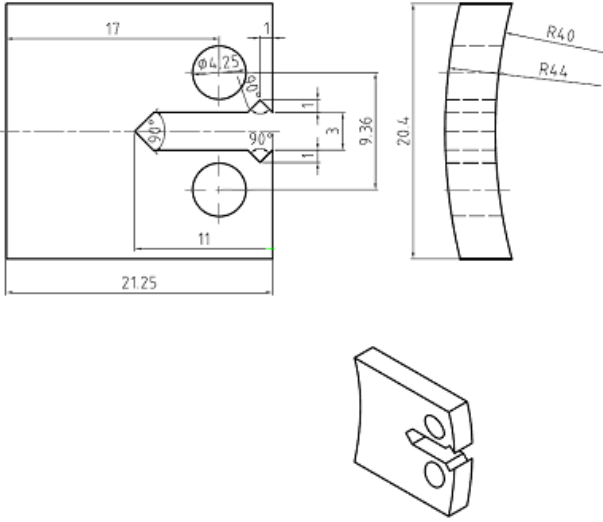


Fig. 5 Compact specimen

Pre-cracking of compact specimens was performed according to the recommendations provided by standards [16]. Testing has been performed supply the requirements [15].

In order to maintain normal tensile stress as perpendicular as possible to the crack growth plane during fracture toughness testing, the grips of compact specimens were subjected by the conical shape pins, which angle was calculated with respect to arch radius of the specimen and initial crack length, which has been pre-cracked on high frequency testing equipment.

Stress intensity coefficient was calculated by the following equation

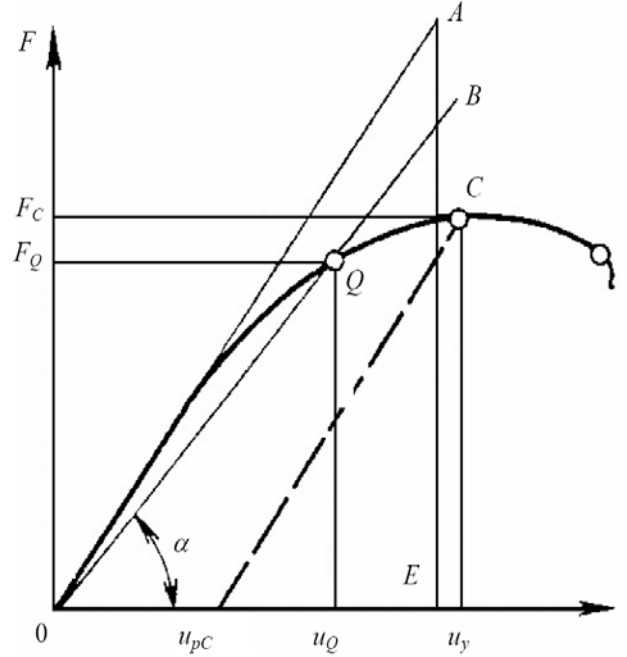
$$K_Q = \frac{F_Q}{B\sqrt{W}} f\left(\frac{a}{W}\right) \quad (1)$$

where  $F_Q$  is the applied load, N;  $B$  is the specimen thickness, m;  $W$  is the specimen width, m;  $a$  is the crack length, m;  $f(a/W)$  was calculated using the equation

$$f\left(\frac{a}{W}\right) = \frac{2 + \frac{a}{W}}{\left(1 - \frac{a}{W}\right)^{3/2}} \left[ 0.866 + 4.64\left(\frac{a}{W}\right) - 13.32\left(\frac{a}{W}\right)^2 + 14.72\left(\frac{a}{W}\right)^3 - 5.60\left(\frac{a}{W}\right)^4 \right] \quad (2)$$

As for all investigated compact specimens  $F_C/F_Q > 1.1$  and  $2.5(K_Q/R_{p0.2})^2$  are higher when  $B$ ,  $a_0$  and  $W - a_0$  calculated stress intensity coefficient  $K_Q$  does not correspond to  $K_{1C}$ . Therefore critical stress intensity coefficient for the specimen of tested thickness  $K_C^*$  was estimated by substituting  $F_Q$  by  $F_C$  in Eq. (2) (Fig. 6).

The estimated stress intensity coefficients are shown in Table 1. The observation of tests showed that stress intensity coefficients decrease with the increase of hydrogen concentration. It is obviously seen from this data, that stress intensity coefficient  $K_C^*$  much more depends on hydrogen concentration than  $K_Q$ .

Fig. 6 Load versus crack displacement of the fourth type curves: scheme of  $F_Q$  and  $F_C$  determinationTable 1  
Fracture toughness characteristics of Zr-2.5% Nb alloy

Hydrogen concentration, ppm	$F_Q$ , N	$F_C$ , N	$K_Q$ , MPa m <sup>1/2</sup>	$K_C^*$ , MPa m <sup>1/2</sup>
0	1950	3580	34	62
45	1800	2890	31	50
95	1720	2880	30	50
137	1810	2610	32	46

### 3. Numerical modelling of the stress intensity factor

The modelling of stress intensity factor for the zirconium alloy without hydrogen and with hydrogen was made using a Finite Element Method (FEM).

The finite element model was prepared for the stress intensity factor modelling (Fig. 7). the FE model was made in consideration of experience of other researchers [17]. Compact specimen 2D FE model's dimensions are the same as the compact specimen dimensions used for the experimental testing (Fig. 5). FE model's initial crack length  $l$  is 1.8 mm (Fig. 8). The two half's of pins were modelled for the transfer of the load. These two half's were meshed with triangles elements. Modelling of the fracture parameters is important that the stress condition was evaluated across the specimen. Stress evaluation across the specimen is obtained using flat continuum 8 nodes QUA8 [18] elements. These elements evaluate the plane strain conditions, i.e. the strain condition evaluates in two directions and the stress condition evaluates in three directions.

The correct size of the mesh is important for finite element models [19]. Especially it is important for modelling of the fracture parameters. The results of the evaluation are acceptable, if the typical elements around the crack tip make the angle, which is in limits from 10° (fine analysis) to 20° (average precision analysis). As shown in the figure 8 the modelled crack tip was meshed with triangular elements that make an angle of 5.5°.

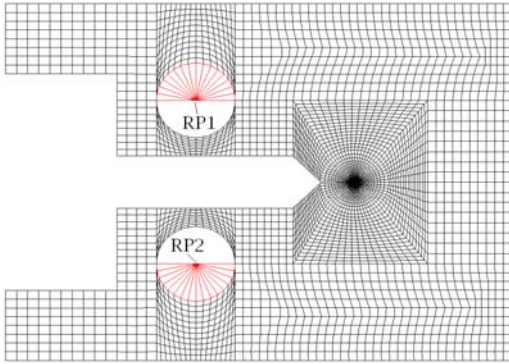


Fig. 7 2D compact specimen finite element model

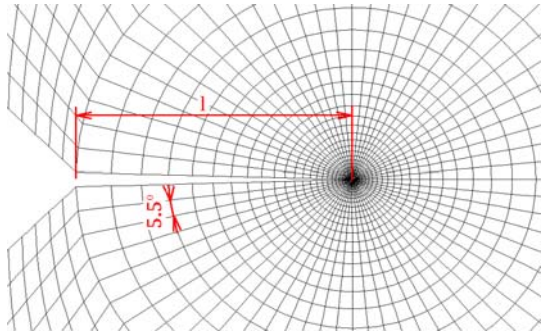


Fig. 8 2D finite element model of the crack tip

The experimentally determined mechanical properties were used for modelling of the stress intensity factor of zirconium alloy with hydrogen and without hydrogen (Fig. 4).

The displacement was used as the load in the modelling of the stress intensity factor. The load was added to the reference point, which was modelled in the centre of the pin (Fig. 7, RP1). The reference point 2 (RP2) was restrained along the X-axis and Y-axis directions.

#### 4. Results of the stress intensity factor study

Analytical analysis of the stress intensity factor of zirconium alloy with hydrogen and without hydrogen was performed using a FEM. Analysis was made at ambient temperature when the concentrations of the hydrogen were 45, 95 and 137 ppm and without hydrogen.

The results of von Mises stresses distribution of zirconium alloy without hydrogen are shown in Fig. 9. As we can see in the figure, the maximum value of stresses is in the crack tip. The stresses reach ultimate strength at the crack tip that means the crack propagation begins. Analogical stresses distribution and fracture character was received for the zirconium alloy with hydrogen concentration of 45, 95 and 137 ppm.

Variation of the tension load with crack opening displacement of the zirconium alloy with hydrogen concentration of 95 ppm is presented in Fig. 10. Crack opening was measured at the load attachment points 1-2 (Fig. 9) as well as during the experiment. It was received reasonably good agreement between predicted and experimental data in elastic region. The stress intensity factor is the parameter of linear fracture mechanics [20]. Therefore the modelling of this parameter can be performed for elastic stress state. The prognosis results of the tension load were compared with testing data at elastic part of loading.

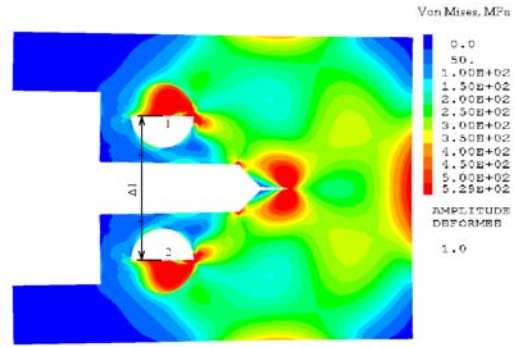


Fig. 9 Distribution of von Mises stresses in the compact specimen area

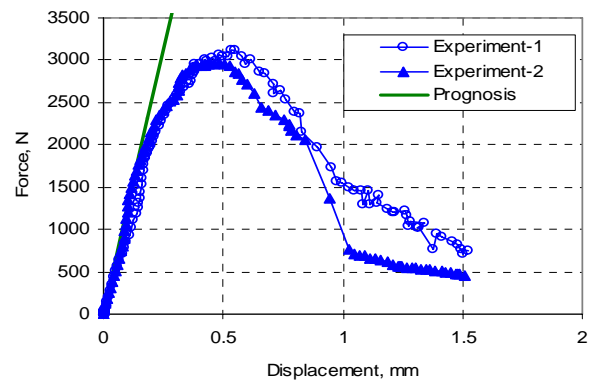


Fig. 10 Variation of the tension load with crack opening displacement of zirconium alloy with hydrogen concentration of 95 ppm

Variations of stress intensity factor with tension load of the zirconium alloy with hydrogen concentration of 95 ppm are presented in Fig. 11. The prognosis results of the stress intensity factor were compared with testing data of the  $K$ , i.e.  $K_Q$  and  $K_C^*$ . Good coincidence of the prognosis results with experimental data was received. Similar results were received in the analysis of zirconium alloy with hydrogen concentration of 45 and 137 ppm and without hydrogen. The deviation of the modelled  $K$  values from experimental  $K_Q$  and  $K_C^*$  do not exceed 6% in case of the analysis of zirconium alloy without and with hydrogen.

The values of calculated and experimentally determined stress intensity factors at different hydrogen concentration are presented in Table 2. The influence of hydrogen concentration on the stress intensity factor is shown in Fig. 12. The continuous and dashed lines present predicted variation of the stress intensity factor with hydrogen concentration received using a FEM and points – experimental data. It is seen that the results of calculated stress intensity factors are between the points of experimental results and they quite good represent the influence of hydrogen on the change of the stress intensity factors. The results of the calculation show that the increase of the volume of hydrogen in the zirconium alloy matrix change the material properties gradually and the existing mismatch to experimental points is caused by the spread of experimental data. The values of calculated and experimentally determined stress intensity factors at different hydrogen concentration are presented in Table 2. It shows that increasing hydrogen concentration from 0 to 137 ppm decreases the stress intensity factor  $K_Q$  by 13% and  $K_C$  decreases by 24%.

Table 2  
Stress intensity factors  $K_Q$  and  $K_C^*$  – modelling result comparison with experiment

Stress intensity factor	Hydride concentration, ppm	Experiment	Prognosis
$K_Q$	0	34	34
	45	31	33
	95	30	31
	137	32	30
$K_C^*$	0	62	59
	45	50	53
	95	50	49
	137	46	48

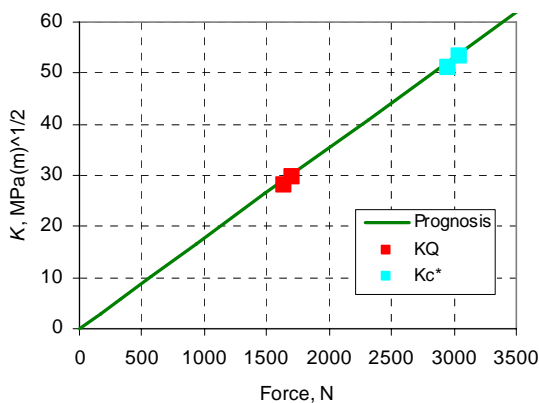


Fig. 11 Variation of stress intensity factor with tension load of zirconium alloy with hydrogen concentration of 95 ppm

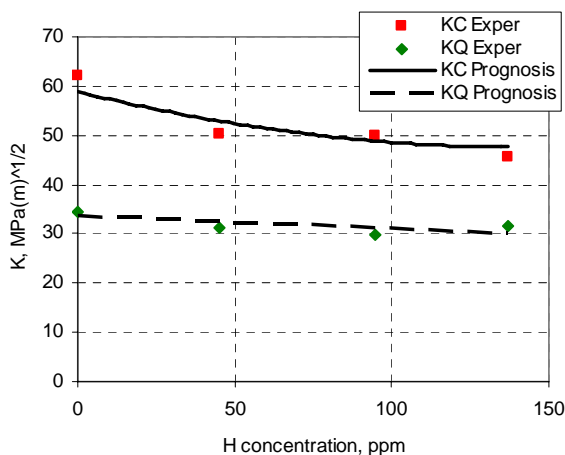


Fig. 12 Variation of stress intensity factor with hydrogen concentration

## 5. Summary and conclusions

The experimental investigation of the hydrogen concentrations influence on mechanical properties was carried out. The obtained mechanical properties for Zr-2.5%Nb alloy at ambient temperature and at different hydrogen concentration showed that increasing of hydrogen concentration causes increasing of yield stress ( $R_{p0.2}$ ) and tensile strength ( $R_m$ ).

The influence of hydrogen concentration on the stress intensity factor was analytically and experimentally evaluated. The modelling of the stress intensity factor of

zirconium alloy (Zr - 2.5% Nb) without and with hydrogen was performed using finite element method. The effect of hydrogen was evaluated by applying experimentally determined material properties to FEM.

Comparison of the stress intensity factor prognosis results of the zirconium alloy with and without hydrogen with experimental data shows that the deviation of calculated stress intensity factors  $K_Q$  and  $K_C^*$  from the experimental values does not exceed 6%. The reason of prognosis result deviation from experimental results is the spread of experimental data. According to prognosis results and experimental data it was determined that increasing hydrogen concentration from 0 to 137 ppm decreases the stress intensity factor  $K_Q$  by 13% and  $K_C^*$  decreases by 24%.

## Acknowledgment

The study was supported by Lithuanian Science Foundation. The authors also would like to express gratitude to the administration and technical staff of Ignalina NPP for providing information regarding operational procedures and operational data.

## References

1. **Almenas, K., Kaliatka, A., Uspuras, E.** Ignalina RBMK-1500. A Source Book.-Lithuanian Energy Institute, 1998.-198p.
2. **Pan, Z.L., Ritchie, I.G. and Puls, M.P.** The terminal splid solubility of hydrogen and deuterium in Zr-2.5Nb alloys.-Journal of Nuclear Materials, 228, 1996, p.227-237.
3. **Coleman, C.E., Hardie, D.** The hydrogen embrittlement of  $\alpha$ -zirconium-A review.-J. of the Less-Common Metals, 1966, 11, p.168.
4. **Bertolino, G., Meyer, G., Perrez Ipina, J.** Mechanical properties at room temperature in ZRY-4 by hydrogen brittleness.-Materials Research, 2002, v.5, No.2, p.125-129.
5. **Kuroda, M., Yamanaka, S., Setoyama, D., Uno, M., Takeda, K., Anada, H., Nagase, F., Uetsuka, H.** Tensile test of hydrided Zircaloy.-J.1 of Alloys and Compounds, 2002, 330-330, p.404-407.
6. **Dubey, J.S., Wadekar, S.L., Singh, R.N., Sinha, T.K., Chakravartty, J.K.** Assessment of hydrogen embrittlement of Zircaloy-2 pressure tubes using unloading compliance and load normalization techniques for determining J-R curves.-J. of Nuclear Materials, 1 January 1999, v.264, Number 1, p.20-28.
7. **Sagat, S., Chow, C.K., Puls, M.P., Coleman, C.E.** Delayed hydride cracking in zirconium alloys in a temperature gradient.-J. of Nuclear Materials, 2000, 279, p.107-117.
8. Delayed hydride cracking in zirconium alloys in pressure tube nuclear reactors, IAEA-TECDOC-1410, 2004.-86p.
9. **Wallace, A.C., Shek, G.K and Lepik, O.E.** Effects of hydride morphology on Zr-. 2.5Nb fracture toughness.-ASTM STP 1023, Zirconium in the Nuclear Industry, ASTM-STP 1023, Eds. L. F. P. Van Swam and C. M. Eucken, ASTM 1989.-66p.
10. **Shia, S.Q, Pulsb, M.P.** Fracture strength of hydride precipitates in Zr-2.5Nb alloys.-J. of Nuclear Materials,

- 1999, 275, p.312-317.
11. **OH, J.Y., KIM, I.S., KIM, Y.S.** A normalization method for relationship between yield stress and delayed hydride cracking velocity in Zr-2.5Nb alloys. -J. of Nuclear Science and Technology, 2000, v.37, No.7, p.595-600.
  12. **Varias, A.G., Massih, A.R.** Simulation of hydrogen embrittlement in zirconium alloys under stress and temperature gradients.-J. of Nuclear Materials, 2000, 279, p.273-285.
  13. **Varias, A.G., Massiha, A.R.** Hydride-induced embrittlement and fracture in metals—effect of stress and temperature distribution.-J. of the Mechanics and Physics of Solids, 2002, 50, p.1469-1510.
  14. **Lepage, A.D., Ferris, W.A., Ledoux, G.A.** Procedure for adding hydrogen to small sections of zirconium alloys.-AECL Report No. FC-IAEA-03, T1.20.13-CAN-27363-03, 1998 November.-16p.
  15. European standard 10002-1. Metallic materials. Tensile testing – Part 1. Method of test at ambient temperatures, 2001.-56p.
  16. GOST 25.506-85. Mechanical test methods of metals. Determination of fracture toughness characteristics under static loading,- Moscow, 1985 (in Russian).
  17. **Žiliukas, A., Meslinas, N., Juzėnas, K.** Fracture investigation of layered composite structural elements. -Mechanika. -Kaunas: Technologija, 2006, Nr.1(57), p.12-16.
  18. **Axisa F.** CASTEM2000: Elements de Theorie et Exemples. Rapport DMT/96-498.-243p.
  19. **Sladkowski, A.** Accuracy analysis of the solution of spatial contact problem by means of the FEM. -Mechanika. -Kaunas: Technologija, 2005, Nr.3(53), p.17-21.
  20. **Anderson, T.L.** Fracture Mechanics. Fundamentals and Applications.-Boca Raton, Ann Arbor, Boston: CRC Press Inc, 1991.-793p.

R. Janulionis, M. Daunys, G. Dundulis, A. Grybėnas,  
R. Karalevičius

#### SKAITINIS IR EKSPERIMENTINIS VANDENILIO ĮTAKOS Zr-2.5%Nb LYDINIO IRIMO TĄSUMO CHARAKTERISTIKOMS TYRIMAS

#### Re z i u m ė

Darbo tikslas – vandenilio įtakos RBMK-1500 reaktoriaus kuro kanalų vamzdžių Zr–2.5%Nb lydinio (TMA–2) irimo tąsumo charakteristikoms eksperimentinis tyrimas bei skaitinis modeliavimas baigtinių elementų metodu. Irimo tąsumo charakteristikų skaičiavimas atliktas remiantis eksperimentiškai nustatytais mechaninėmis cirkonio lydinio savybėmis, esant vandenilio kiekiui iki 137 ppm. Gautus skaičiavimo rezultatus palyginus su eksperimentiniais duomenimis, nustatyta, kad apskaičiuotų įtempių intensyvumo koeficientų  $K_Q$  ir  $K_C^*$  reikšmės, taip pat jų priklausomybės nuo vandenilio koncentracijos yra tarp eksperimentinių taškų. Įskaitant eksperimentinių rezultatų sklaidą, jų nuokrypis nuo skaičiavimo rezultatų neviršija 6%. Buvo nustatyta, kad, padidėjus vandenilio koncentracijai cirkonio lydinyje iki 137 ppm, esant 20°C,

įtempių intensyvumo koeficientas sumažėja 13%, o  $K_C^*$  – 24%.

R. Janulionis, M. Daunys, G. Dundulis, A. Grybėnas,  
R. Karalevičius

#### NUMERICAL AND EXPERIMENTAL RESEARCH OF THE INFLUENCE OF HYDROGEN TO THE FRACTURE TOUGHNESS OF ZIRCONIUM – 2.5% NIOBIUM ALLOY

#### S u m m a r y

The aim of work was the experimental investigation and numerical modelling using finite element method of influence of hydrogen to the fracture toughness of Zr-2.5 Nb alloy of a pipe of the fuel channel with TMT-2 reactor RBMK-1500. Calculation of characteristics of fracture toughness was made with use of experimentally determined mechanical properties of zirconium alloy containing hydrogen up to 137 ppm. Comparison of the received results of calculation with experimental data has shown, that the calculated intensity factors  $K_Q$  and  $K_C^*$ , and also their dependences on concentration of hydrogen are between experimental points. Including the spread of experimental results, their deviation from calculated data does not exceed 6%. It was determined, that the increase in of hydrogen concentration up to 137 ppm at 20°C decreases the value of intensity factor  $K_Q$  by 13% and  $K_C^*$  by 24%.

Р. Янулёнис, М. Даунис, Г. Дундулис, А. Грибёнас,  
Р. Каралевичюс

#### ЧИСЛОВОЕ И ЭКСПЕРИМЕНТАЛЬНОЕ ИССЛЕДОВАНИЕ ВЛИЯНИЯ ВОДОРОДА НА ВЯЗКОСТЬ РАЗРУШЕНИЯ ДЛЯ СПЛАВА Zr-2.5%Nb

#### Р е з ю м е

Целью работы явилось экспериментальное исследование и числовое моделирование методом конечных элементов влияния водорода на вязкость разрушения сплава циркония Zr-2.5 Nb трубы топливного канала с ТМО-2 реактора RBMK-1500. Расчет характеристик вязкости проводился с использованием экспериментально определенных механических свойств циркониевого сплава, содержащего до 137 ppm водорода. Сравнение полученных результатов расчета с экспериментальными данными показало, что рассчитанные коэффициенты интенсивности напряжений  $K_Q$  и  $K_C^*$ , а также их зависимости от концентрации водорода находятся между экспериментальными точками. Включая разброс экспериментальных результатов, их отклонение от расчетных данных не превышает 6%. Определено, что увеличение концентрации водорода до 137 ppm при 20°C снижает значение коэффициента интенсивности  $K_Q$  на 13%, а  $K_C^*$  – на 24%.

Received October 13, 2008

Accepted November 04, 2008